# THIN FILM INTERMEDIATE BAND CHALCOPYRITE SOLAR CELLS: THEORETICAL ANALYSIS OF DEVICE PERFORMANCE AND PROSPECTS FOR THEIR REALISATION

David Fuertes Marrón, Antonio Martí, César Tablero, Elisa Antolín, Enrique Cánovas, Pablo García Linares, Antonio Luque
Instituto de Energía Solar – ETSIT. Universidad Politécnica de Madrid
Ciudad Universitaria s.n., 28040 Madrid, Spain.

ABSTRACT: The feasibility of implementing the intermediate-band (IB) concept into a relevant thin-film technology has been assessed. Compounds belonging to the group of I-III-$VI_2$ chalcopyrites, currently used as absorbers in the leading thin-film technology, appear as promising candidates for the realization of IB-devices. In this paper we first analyze the expected performance of such a thin-film intermediate band solar cell (TF-IBSC) by considering different levels of idealization. In the second part of the paper some issues relevant for the practical realization of IBs in chalcopyrites are discussed and impurities acting as potential IB-precursors in the chalcopyrite sulfide host identified.
Keywords: Intermediate band; thin-film solar cells; chalcopyrites

## 1 INTRODUCTION

The intermediate band (IB) concept [1] has attracted attention as a means of surpassing the theoretical conversion efficiency limitations of conventional solar cells [2]. Experimental evidences of the working principle of IBs have been reported recently [3], yet the efficiency figures achieved by current devices lag behind the theoretical expectations. Such currently used IB-devices are based on quantum-dot intermediate band solar cells (QD-IBSC) made of III-V semiconductor compounds and alloys by epitaxial-growth methods. This technology is well established and provides high-quality materials for opto-electronic applications, although its use for mass PV-production will likely require the use of light concentration schemes. From this perspective, it appears meaningful to quest for an alternative technology that can profit from the IB concept while meeting the target of reducing the processing time and the costs associated to wafer-based technologies. Thin-film (TF) solar cells are attractive candidates for this purpose.

TF solar cells based on $Cu(In,Ga)Se_2$ chalcopyrite absorbers are approaching 20% conversion efficiency at laboratory scale [4] and stepping firmly into industrial production. Comprehensive reviews on chalcopyrite-based solar cell technology can be found elsewhere [5]; here we will only point out a few remarkable properties of semiconductors of the type I-III-$VI_2$ of relevance for the following discussion, such as (i) tolerance of the electronic quality with respect to high concentrations of native defects; (ii) a generally benign electronic behaviour of grain boundaries in microcrystalline material as used for cells; (iii) adjustment of the bandgap of the compound between 1.0 eV for $CuInSe_2$ up to 3.4 eV for $CuAlS_2$ upon alloying different ratios of elements of groups IIIa and VIa; and (iv) forgiveness of material processing. All these issues make chalcopyrites highly attractive for the realization of TF-PV devices and promising hosts for IBs.

## 2 EVALUATION OF DEVICE PERFORMANCE

The evaluation of the potential efficiency limits of a TF-IBSC has been carried out at different levels of idealization. We will first refer to the ideal case, which imposes absolute limits as set by the detailed balance theory. We will further discuss the results obtained when including certain non-idealities in the model, which should bring the calculated efficiencies down to more realistic figures. The aim in this respect is to include in the IB-model important experimental observations made on current conventional devices that are known to limit their performance. We will mention in the following four of these sources of non-idealities: current losses, the impact of non-radiative recombination, the diode contribution, and a particular case of incomplete selectivity of the absorption coefficients. At the end of this section these contributions will be explicitly included in the numerical model of the TF-IBSC.

### 2.1 Ideal performance

The TF-IBSC is expected to operate under one-sun irradiation, as for conventional TF-technologies. Its maximum theoretical efficiency has been calculated accordingly by considering a non-concentrated illumination source corresponding to a black-body at 6000 K, about the temperature of the sun's photosphere. The calculations for the ideal performance have followed the detailed balance approach, assuring selective and full absorption at the three possible electronic transitions permitted by the IB-material (valence-to-intermediate-, intermediate-to-conduction-, and valence-to-conduction-band), as well as a complete collection of photogenerated carriers with no resistive losses.

Figure 1 shows the calculated theoretical efficiencies as a function of the main gap of the host semiconductor for both conventional single-gap devices and the IB-counterparts operated both at one sun [6]. For the case of the TF-IBSC, the optimal position of the IB has been considered for each value of the main gap in the left panel of the figure. It can be observed that, while the efficiency of the single gap device is limited at about 31% for a gap close to 1.4 eV, the TF-IBSC approaches 47% for a gap value of 2.4 eV. Both curves cross each other at 1.14 eV. For gap values above this energy, the TF-IBSC is expected to outperform the single-gap device, whereas no net gain is predicted by the incorporation of an IB in single gap devices for values of the gap below 1.14 eV. This particular energy gap is of special interest in conventional chalcopyrite-based technology, as it corresponds to the gap of absorbers from which the high-efficiency devices based on $Cu(In_{0.7}Ga_{0.3})Se_2$ are fabricated. Further details of the

analysis of the expected device performance of a TF-IBSC with 1.14 eV bandgap can be found in [6], the main conclusions being that, although minor, an improvement of the efficiency is to be expected when considering some non-idealities, as discussed in a similar fashion in the following for widegap compounds. The black dots superimposed on the efficiency curve for TF-IBSCs in Figure 1 correspond to the nominal gaps of non-alloyed chalcopyrite compounds $CuInSe_2$, $CuInS_2$, $CuGaSe_2$ and $CuGaS_2$, although it should be mentioned that the entire curve can be spanned by alloying different ratios of group-III- and group-VI-elements (In-Ga and S-Se, respectively). Pure $CuGaS_2$, with a bandgap about 2.46 eV, appears close to the optimum bandgap for the realization of TF-IBSCs, and has been proposed before as a candidate for hosting an IB [6,7].

The right panel of Figure 1 shows the dependence of the calculated maximum efficiency of a TF-IBSC on the relative position of the IB with respect to either the valence or conduction band [1]. It can be observed that for all chalcopyrite compounds considered with a bandgap above the critical value of 1.14 eV, a similar dependence is found: the efficiency curves peak asymmetrically around an optimum value for each compound (0.45 eV for $CuInS_2$, 0.54 eV for $CuGaSe_2$, and 0.92 eV for $CuGaS_2$) with maxima off midgap values, whereas for the low-gap compound $CuInSe_2$ the maximum efficiency is predicted for a IB overlapping the band edge (i.e., no IB present). This result implies that a minimum gap of the host material is required for the device to profit from the presence of an IB. If this requirement is not fulfilled, the recombination associated to transitions involving the IB, while only considered of radiative nature, overcompensates for any potential gain in photogenerated current assisted by the IB.

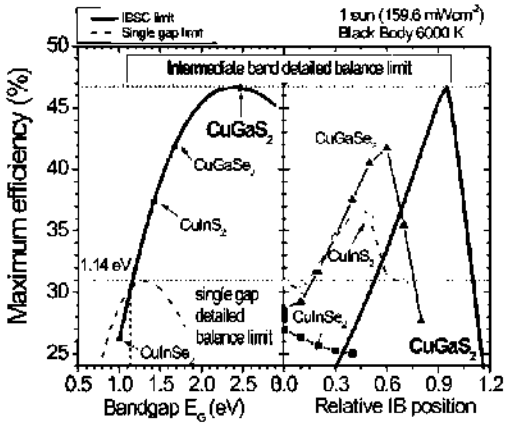


**Figure 1**: (Left) Maximum theoretical efficiency calculated within the detailed balance theory under one-sun illumination from a black-body at 6000 K of a conventional single gap solar cell (dashed) and the ideal intermediate band counterpart (solid). Horizontal dotted lines mark the respective highest efficiencies calculated. (Right) Efficiency as a function of the relative position of the IB for the cases of $CuInSe_2$ (solid squares), $CuInS_2$ (open circles), $CuGaSe_2$ (solid triangles) and $CuGaS_2$ (solid line).

2.2 Current losses

The experimental photocurrent obtained from single gap, chalcopyrite-based devices does not correspond to the theoretical maximum that could be expected from the value of the gaps of the corresponding absorbers. A number of factors contribute to these current losses, like a finite reflectance over the optical wavelength range of the incoming radiation, an incomplete collection of photogenerated minority carriers, shading of the front contact grid, etc. In order to perform a fair comparison between experimental devices and the idealized TF-IBSC, we have included a factor (CL) of current losses in the IB-model that reflects the current state of the art of the corresponding IB-free devices. For the case of low-gap $Cu(In_{0.7}Ga_{0.3})Se_2$ these losses are estimated at 23% [5], going up to about 35% for the wide-gap compound $CuGaSe_2$. These estimations have been made comparing the reported photocurrents of record devices [4,8] with the theoretically obtainable value for a given bandgap under standard illumination conditions. Therewith, we have assumed that the incorporation of the IB does not imply any improvement of the device in this regard.

2.3 Diode contribution

The electronic transport in conventional chalcopyrite-based devices is characterized by an ideality factor of the associated single-diode equivalent circuit m>1 at room temperature [1.14 for $Cu(In_{0.7}Ga_{0.3})Se_2$ and 2.1 for $CuGaSe_2$, from Refs. 4, 8] which speaks for devices limited by non-radiative recombination via states in the gap, likely assisted by tunneling as the gap increases. The ideality factor, together with the corresponding saturation current of the reported best-performing devices, has been considered in the TF-IBSC model, by including a diode term in the related equations of the total current.

2.4 Non-radiative recombination

Conventional chalcopyrite-based devices do not operate in the radiative limit, as requested for maximum theoretical efficiencies under the detailed balance approach. Furthermore, it would be realistic to consdider that the IB, though performing close to ideality, would have to compete with intrinsic non-radiative recombination mechanisms operating in the semiconductor host. In order to establish the tolerance of the TF-IBSC to non-radiative recombination we have included a *non-radiative factor* (NRF) in the model, defined as the unity plus the ratio of the magnitudes of non-radiative to radiative recombination processes. In this fashion it is possible to estimate the impact of the non-radiative contribution on the performance of the device by varying its relative magnitude [9].

2.5 Overlapping absorption coefficients

A further restriction of the original IB-theory refers to the selective character of the electronic transitions involved in the operation of the IBSC as a function of the energy of the incoming photons. The effects on the expected performance of IB-devices due to non-idealities of the absorption coefficients have been studied in detail [10] and here we just focus on one particular case. We will consider that the absorption coefficients related to transitions VB→IB and IB→CB overlap over the energy range $E_L<E<E_H$, where $E_L$, $E_H$ refer to the two transition energies the main bandgap is divided into by the presence of the IB. Furthermore, the same magnitude for the two absorption coefficients involving the IB is considered, while for energies $E \geq E_G$ the associated

transitions VB→CB dominate the absorption processes. This example reflects the case in which the IB presents a finite width and a low absorption coefficient compared to the corresponding absorption processes not involving the IB. It can be shown that for this case the total current of the device can be expressed as [6,9]:

$$\frac{J}{q} = [\dot{N}(E_L, E_H, 0, T_{sun}) + \dot{N}(E_G, \infty, 0, T_{sun}) + \\ + \frac{1}{2}\dot{N}(E_H, E_G, 0, T_{sun})](1 - \mathbf{CL}) - \\ - \mathbf{NRF}[\dot{N}(E_L, E_H, \mu_{IC}, T_{cell}) + \dot{N}(E_G, \infty, V, T_{cell}) + \\ + \frac{1}{4}\dot{N}(E_H, E_G, \mu_{IC}, T_{cell}) + \frac{1}{4}\dot{N}(E_H, E_G, \mu_{IV}, T_{cell})] - \\ - \mathbf{J_0}\left(e^{\frac{qV}{\mathbf{m}kT}} - 1\right)$$

where the previously discussed corrections have also been included (CL: current losses; NRF: non-radiative factor; $J_0$,m: diode parameters). In this equation, $\dot{N}$ represents the photon flux in a given energy range as a function of the temperature of the light source and the chemical potential of the radiation (or the splitting of quasi-Fermi levels for the radiative transitions involved); $E_L$, $E_H$, $E_G$ represent the three gaps of the IBSC. The first three terms of the equation account for generation processes ending up with free electrons at the CB (a similar expression holds for holes at the VB). The factor CL corrects, as discussed before, for the fact that experimental devices are not able to extract the entire amount of photocurrent they could potentially generate. The next four terms in the expression account for recombination processes as required by the detailed balance theory, and they are weighted with the factor NRF accounting for the eventual existence of recombination processes in addition to those purely radiative: NRF=1 represents the radiative case and NRF>1 allows for non-radiative recombination by considering the respective magnitudes of both types of processes. It should be mentioned that the model could also account for different ratios of both types of recombination events controlling each transition separately, for instance if non-radiative recombination dominates one of the possible electronic transitions, the others being mainly of radiative character, but for the sake of clarity we do not further consider this point here. Finally, the diode term includes the saturation current and the ideality factor that help comparing performances of idealized IBSC and real cells. Two additional equations, ensuring no net charge accumulation taking place at the IB and linking the external voltage bias with the splitting of the quasi-Fermi levels for the valence and conduction bands allow calculating I-V curves of the IBSC for a given illumination level [1].

### 2.6 A case of study: $CuGaSe_2$-based TF-IBSC

As discussed before, widegap chalcopyrites are expected to profit from IBs to a larger extent than lowgap counterparts. Whereas $CuGaS_2$ appears as the absorber of choice for TF-IBSC, no operative solar cells have been reported from this absorber due to its large bandgap (although it has been studied as for light-emitting diodes and lasers [11]). The next non-alloyed chalcopyrite compound with a lower gap is $CuGaSe_2$, for long time being the candidate of choice for an eventual top-cell in tandem structures [5]. We have chosen this absorber as the host of a TF-IBSC, for we count with experimental reported performance of conventional single gap devices to compare our results with.

The results of the model discussed above for the case of a TF-IBSC based on $CuGaSe_2$ hosting an IB at the ideal position within the main gap (i.e. some 0.57 eV away from either the VB or CB) are summarized in Table I. In these calculations we have assumed that the diode-related properties of the TF-IBSC are given by the current state of the art of $CuGaSe_2$-based devices. In particular, *CL* is set at 0.35 and $J_0$ and *m* at $7.0\times10^{-7}$ mA/cm$^2$ and 2.1, respectively [8]. We have compared the best reported performance under AM1.5G illumination of a conventional $CuGaSe_2$ cell with that expected from the corresponding TF-IBSC. For this purpose we have first calculated the equivalent results under black-body radiation at 6000 K of the AM1.5 results, labeled as *BB-equivalent* in the last row of Table I [6].

**Table I:** Calculated performance of a TF-IBSC device based on $CuGaSe_2$ host material including the non-idealities discussed in the text, in all cases CL=0.35, $J_0=7.0\times10^{-7}$ mA/cm$^2$, m=2.1, compared to the best performance reported for a conventional $CuGaSe_2$-based solar cell, last two rows in italics [8].

| | **NRF** | **$J_{sc}$** | **$V_{oc}$** | **η** |
|---|---|---|---|---|
| Radiative | 1 | 40.09 | 970 | 19.3 |
| | $10^2$ | 40.09 | 940 | 19.1 |
| Non-radiative | $10^3$ | 40.09 | 854 | 17.4 |
| losses allowed | $10^4$ | 40.07 | 741 | 14.7 |
| | $10^5$ | 39.90 | 622 | 11.9 |
| α-overlap | 1 | 31.71 | 957 | 15.0 |
| *Exp. AM1.5* | | 14.88 | 905 | 9.5 |
| *BB-equivalent* | | 23.33 | 940 | 10.8 |

From these results it is concluded that, as expected, non-idealities will play a central role in the performance of IBSC devices. Allowing for current losses and for a diode term, as for the current state-of-the-art device, brings the efficiency figures for $CuGaSe_2$-based TF-IBSC from an ideal 42% down to 19.3%. The eventual overlapping of absorption coefficients in the manner discussed above will further reduce the efficiency to 15%, mainly due to a reduced photocurrent. Nevertheless, these figures reflect a relative improvement of the efficiency of some 80% and 40%, respectively, with respect to the experimental reports for a single gap device. Accounting for non-radiative recombination in turn imposes limitations on the output voltage. It is of particular interest to monitor the expected performance of the device as a function of the NRF, as this number can be considered as a direct indicator of the tolerance of the solar cell with respect to non-radiative losses. It is concluded that for NRF values as high as $10^5$, the TF-IBSC device still outperforms its single-gap counterpart, though at reduced operating voltages.

## 3 INTRODUCING IBs IN CHALCOPYRITES

The first suggested approach toward the realization

of IB-chalcopyrite compounds has been the introduction of large amounts of a few foreign transition-metal elements at substitutional places of the cation sub-lattice [7]. The resulting electronic structure has been calculated numerically. In most cases, the states around the Fermi energy associated with the impurity species overlap states of the host at either the conduction or the valence band, being therefore not suitable for IBs. However, for particular cases, the resulting density of electronic states includes isolated bands within the bandgap of the host. Generally speaking, the density of states (and, to a lesser extent, also its energy position within the gap) depends on the concentration of impurities considered. This turns out to be a critical issue, as, on the one hand, the solubility of impurity species in a given crystalline host is normally limited, and on the other hand, a significant concentration of impurities in the atomic percentage range might be required for operating IB-devices [12].

The most reliable method in order to predict the existence of an IB in the chalcopyrite host resulting from the substitution of certain cations by selected impurities is to perform computing-demanding calculations of the electronic structure out from first principles [7]. In order to widen the scope of reported results on potential candidates leading to IBs while optimizing resources, a first elemental screening has been carried out, whereby thermo-chemical arguments have helped classifying the impurity candidates prior to the realization of full electronic-structure calculations on the most promising ones. The classification followed after comparing the enthalpies of formation of the ternary host with the corresponding enthalpies of potential competing phases built up by the reaction of the intended impurities with the constituent chalcogen of the host, as in [13]. For $CuGaS_2$, identified before as an optimal candidate to hosting an IB, $\Delta H_f^0$=-2.49 eV/at [13]. Thermo-chemical data of a number of binary chalcogenides can be found, for example, in Ref. [14]. The existence of other stable solid phases (only binary compounds have been considered) imposes restrictions on the range of existence of the ternary chalcopyrite through their respective chemical potentials and stoichiometry coefficients. This issue appears particularly relevant when attempting to grow IB-TFs. Chalcopyrite thin films are usually grown in multistage processes, in which the stochiometry of the film undergoes changes, different crystalline phases coexist at certain stages, and the chalcogens used as constituents are provided in excess during a significant fraction of the processing time [5]. It is thus expected that the incorporation of at least one additional elemental species during the growth of the film may alter the complex thermo-chemical equilibrium of the material system. Anticipating where the main sources of conflict in terms of material stability may appear is of major importance for experimentalists attempting to grow TF-IBs.

Following the procedure outlined above, the studied elements have been classified in three categories, namely (i) those for which eventual competing binary chalcogenides are not expected to inhibit the growth of the modified chalcopyrite; (ii) those for which difficulties are foreseen in this respect; and (iii) elements for which no reliable data could be found that helped elucidate on this issue. Calculations of the electronic structure have been subsequently carried out within the frame of the density functional theory (DFT) on those candidates for which no inhibition is predicted and for selected cases for which no reliable data could be found. From the complete analysis of the results, it appears that impurities of the groups VIII-b and IV-a of the periodic table have potential to introduce an IB that could be operative in a TF-IBSC device based on $CuGaS_2$. More details about the calculation procedure and the energetics of the substitutional systems (whether the impurities would find it energetically favorable to enter the chalcopyrite structure or not) will be published elsewhere [15].

## 4 CONCLUSIONS

The potential efficiency gain to be expected from thin-film intermediate band solar cells has been discussed in comparison to conventional single gap devices with current state-of-the-art performance. The comparative analysis demonstrates the importance of non-idealities like current losses, diode factor, non-radiative recombination and failure of complete selectivity of the absorption coefficients involved in the operation of an IBSC, while still predicting a significant gain in efficiency figures upon implementation of an IB. Theoretical calculations have been carried out in this last respect in order to screen interesting candidates for this purpose.

This work has been supported by the European Commission, the Spanish National Programme, and the Comunidad de Madrid under the contracts IBPOWER (211640), GENESIS FV (CSD2006-00004), and NUMANCIA (S-0505/ENE000310), respectively. DFM acknowledges financial support from the Spanish Ministry of Science and Innovation within the program Ramón y Cajal.

## REFERENCES

[1] A. Luque, A. Martí, Phys. Rev. Lett. 78 (1997) 5014.
[2] W. Shockley, H.J. Queisser, J. Appl. Phys. 32 (1961) 510.
[3] A. Martí *et al.*, Phys Rev. Lett. 97 (2006) 247701.
[4] I. Repins *et al.*, Prog. Photovolt: Res. Appl. 16 (2008) 235.
[5] See, for example, W.N. Shafarman and L. Stolt, *Handbook of PV Science & Eng*, Wiley (2003), 567.
[6] A. Martí, D. Fuertes Marrón, A. Luque J. Appl. Phys. 103 (2008) 073706.
[7] P. Palacios *et al.*, Thin Solid Films 515 (2007) 6280.
[8] D.L. Young *et al.*, Prog. Photovolt: Res. Appl. 11 (2003) 535.
[9] D. Fuertes Marrón, A. Martí, A. Luque, Thin Solid Films, in press.
[10] L. Cuadra, A. Martí, A. Luque, IEEE Trans. Electr. Dev. 51 (2004) 1002.
[11] J.L. Shay, B. Tell, H.M. Kasper, Appl. Phys. Lett. 19 (1971) 366.
[12] A. Luque *et al.*, Phys. B 382 (2006) 320.
[13] Y.-J. Zhao, A. Zunger, Phys. Rev. B 69 (2004) 075208.
[14] O. Knacke, O. Kubaschewski, K. Hesselmann, *Thermochemical Properties of Inorganic Substances*, Springer (1991).
[15] C. Tablero, D. Fuertes Marrón, submitted.